Electrical control of the exciton–biexciton splitting in self-assembled InGaAs quantum dots

M Kaniber[1], M F Huck[1], K Müller[1], E C Clark[1], F Troiani[2], M Bichler[1], H J Krenner[3] and J J Finley[1]

[1] Walter Schottky Institut, Technische Universität München, Am Coulombwall 4, 85748 Garching, Germany
[2] S3, Instituto Nanoscienze-CNR, 41125 Modena, Italy
[3] Lehrstuhl für Experimentalphysik 1 and Augsburg Center for Innovative Technologies (ACIT), Universität Augsburg, Universiätsstr. 1, 86159 Augsburg, Germany

E-mail: kaniber@wsi.tum.de

Abstract
The authors demonstrate how lateral electric fields can be used to precisely control the exciton–biexciton splitting in InGaAs quantum dots. By defining split-gate electrodes on the sample surface, optical studies show how the exciton transition can be tuned into resonance with the biexciton by exploiting the characteristically dissimilar DC Stark shifts. The results are compared to model calculations of the relative energies of the exciton and biexciton, demonstrating that the tuning can be traced to a dominance of hole–hole repulsion in the presence of a lateral field. Cascaded decay of the exciton–biexciton system enables the generation of entangled photon pairs without the need to suppress the fine structure splitting of the exciton. Our results demonstrate how the exciton–biexciton system can be electrically controlled.

The controlled generation of entanglement is an important concept in both quantum information science [1] and quantum cryptography [2]. Benson *et al* [3] proposed the use of the biexciton–exciton ($2X^0$–$1X^0$) cascade in semiconductor quantum dots (QDs) to generate entangled photon pairs. Subsequently, a number of groups [4–6] have demonstrated the generation of entangled photon pairs via this process. Creating polarization entangled, rather than classically correlated [7], photon pairs has been achieved by tuning the exciton fine structure splitting to zero [8]. Recently, this has been achieved by several groups [9–12] by applying an electric field in a lateral geometry in the base plane of the QD. An alternative approach for realizing an entangled photon source, proposed by Avron *et al* [13], requires the $1X^0$ to be tuned into resonance with the $2X^0$ in order to exploit time reordering of the emitted photon pair.

In this paper we demonstrate tuning of $1X^0$ and $2X^0$ states of single InGaAs QDs into resonance by applying an electric field in the basal plane of the QDs [14]. Comparison with theory shows that the sign of the DC Stark shift [15] is opposite for both transitions to be tuned into resonance at low electric fields ($F \sim 17$ kV cm^{-1}). Such devices are promising for realizing sources of entangled photon pairs with electrical control of the entanglement.

The samples investigated were grown by molecular beam epitaxy and consist of the following layer sequence: starting with a semi-insulating (100) GaAs wafer we deposited a 300 nm thick GaAs buffer layer, followed by 25 periods of a AlAs (2.5 nm)/GaAs (2.5 nm) superlattice. We grew a 200 nm thick GaAs waveguide, into the center of which a single layer of nominally $In_{0.5}Ga_{0.5}As$ QDs was incorporated. The areal density of the QDs was varied during the growth by stopping the rotation of the wafer and samples with a density of $\sim$10 μm^{-2}, as revealed by atomic force microscope measurements (not shown here), were chosen for further processing. Using a combination of optical lithography and electron beam metallization we established back-to-back Ti/Au Schottky gates on the surface of the sample. In the inset of figure 1(c) we present an optical microscope image of a fabricated device showing the split-gate contacts, labeled I

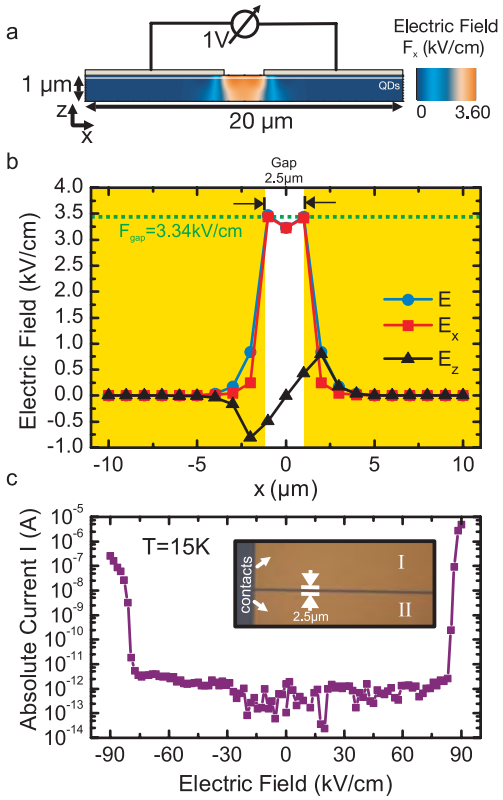

Figure 1. (a) Simulated electric field distribution for the split-gate geometry for an applied voltage of 1 V. (b) Simulated electric field at the QDs (100 nm below the sample surface) for the x-component (squares), z-component (triangles) and the total electric field (circles). (c) Current as a function of applied electric field for a back-to-back Schottky diode at $T = 15$ K without illumination. Inset: top view photograph of a completely processed sample with a 2.5 μm wide gap.

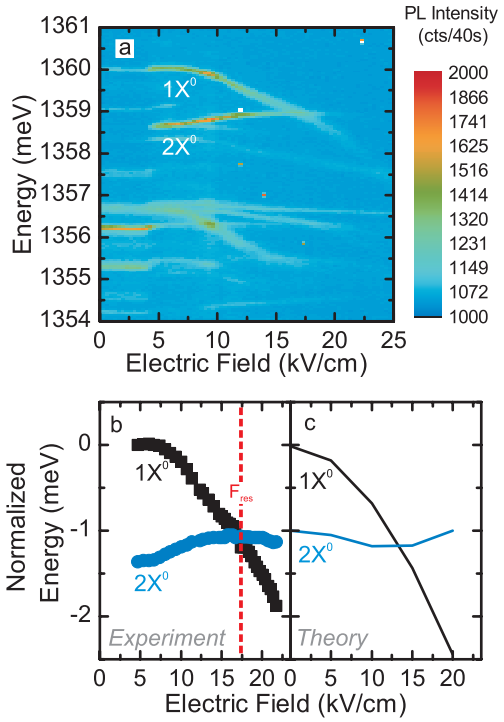

Figure 2. (a) PL spectra recorded as a function of electric field from 0 to 25 kV cm^{-1} (false color plot). (b) Extracted normalized energy of the emission lines $1X^0$ and $2X^0$ as a function of electric field resulting in a resonance at $F_{res} \sim 17$ kV cm^{-1}. (c) Calculations of the renormalization energies of the $1X^0$ and $2X^0$ lines of a single QD in a lateral electric field geometry.

and II, separated by a 2.5 μm wide gap. We simulated the electric field distribution between the contacts I and II using finite element simulations (QuickField see [16]) that solve the three-dimensional Poisson equation for a given geometry with appropriate boundary conditions. The result of the simulation for our contact geometry with an applied potential set to 1 V is presented in figure 1(a). The electric field is encoded in a false color representation and the position of the QD layer is indicated by the white line, ∼100 nm below the sample surface. The electric field within the gap between the contacts and in the region of the QD is homogeneous and almost entirely oriented in the (x, y) plane. This can be seen from figure 1(b) that shows the electric field in the lateral (x)- and vertical (z)-direction as a function of the distance from the gap center. From this simulation we established the relationship between V_{app} and the electric field, obtaining $F_{gap} = 3.34$ kV cm^{-1}. A typical current–voltage characteristic recorded from our samples at $T = 15$ K without illumination is presented in figure 1(c). This clearly shows that the devices fabricated have very low leakage currents <1 pA, for lateral electric fields in the interval -75 to $+75$ kV cm^{-1}. This indicates excellent current blocking of the back-to-back Schottky contacts, allowing us to apply lateral electric field perturbations to the QD whilst simultaneously interrogating them optically.

The optical studies were performed using a confocal micro-photoluminescence (μ-PL) setup that provides a spatial resolution of ∼700 nm at emission wavelength 950 nm. The sample was mounted in a helium-flow cryostat to achieve $T = 15$ K and electrically connected to a programmable voltage source. The sample was excited quasi-resonantly, via the wetting layer ($E_{ex}^{WL} = 1.46$ eV) using a continuous wave Ti:sapphire laser. The PL signal arising from single QDs was collected using an 100× microscope objective (numerical aperture = 0.8), spectrally dispersed by a 0.55 m imaging monochromator and detected with a Si-based, liquid nitrogen cooled charge coupled device detector.

In figure 2(a) we present typical μ-PL measurements of a single QD as a function of applied electric field in the field range 0 to +25 kV cm^{-1} as a false color plot. Two dominant emission peaks are observed for electric fields $F >$ 4.5 kV cm^{-1}, labeled $1X^0$ ($E_{1X^0} = 1360.02$ meV) and $2X^0$ ($E_{2X^0} = 1358.66$ meV), respectively. These lines are attributed to the single neutral exciton and biexciton, respectively (see discussion below). For electric fields in the range 0 kV cm^{-1} < F < 4.5 kV cm^{-1}, the spectrum is dominated by a complex series of emission lines that are shifted in energy and abruptly quench when the critical field, $F_{crit} = 4.5$ kV cm^{-1}, is reached. As discussed below, we attribute this behavior to the appearance of charged states in the QD due to field induced ionization of excitons pumped into the wetting layer

and non-germate electron–hole (e–h) carrier capture into the dot [17]. This gives rise to many emission lines due to statistical fluctuations of the charge status of the dot.

For electric fields $F > 4.5$ kV cm^{-1} the emission energy of $1X^0$ decreases as expected whilst the emission energy of $2X^0$ increases. This behavior is attributed to the quantum confined Stark effect [15]. For the $1X^0$ state the final state is an empty QD. Therefore, the observed Stark shift is completely determined by the field induced modification of the Coulomb interaction between the electron and hole, V^{eh}. This results in a quadratic Stark shift toward lower energy according to [15]

$$E = E_0 - \beta_{1X^0} \cdot \vec{F}^2 \qquad (1)$$

where E_0, β_{1X^0} and $\vec{F}$ denote the exciton energy at zero electric field, the polarizability of the e–h pair and the applied electric field, respectively.

The strongly different DC Stark shift of the $2X^0$ line compared to $1X^0$ results primarily from the repulsive Coulomb interaction between the two holes or/and the two electrons in the $2X^0$ that are not compensated by the attractive 2e–2h interaction. This effect appears predominantly for lateral electric fields since the electric field is applied parallel to the base of the QDs which is typically ∼30 nm and, therefore, much larger than its height of typically ∼5 nm [18]. The opposing DC Stark shift allows the $1X^0$ and $2X^0$ lines to be tuned into resonance at an electric field $F_{res} \sim 17$ kV cm^{-1}, as shown in figure 2(b). Further increase of the electric fields tunes the $1X^0$ and $2X^0$ out of resonance once again. At large applied fields we observe a pronounced decrease of the PL intensity due to a combination of suppressed charge carrier capture into the QDs from the wetting layer and enhanced carrier tunneling escape out of the QD.

To support these ideas we calculated the DC Stark shift of the $1X^0$ and $2X^0$ states in a QD. The calculations were performed by considering a three-dimensional disc-shaped potential ($V = 0$ in the disc and $V = V_0$ outside the disc) that reflects the nominal dimensions of the quantum dot and includes Coulomb interactions via a configuration interaction approach. The dimensions of the disk in the model have been fixed after the nominal dimension of the dot. Fine tuning of the disk dimension has been achieved by fitting the observed spectrum. The effects we discuss are robust with respect to small variations of the disk size. In figure 2(c) we present calculations of the renormalization energies of the $1X^0$ and $2X^0$ lines for a disc-shaped InGaAs/GaAs QD (base length 18 nm and height 4 nm) as a function of electric field. In order to calculate the transition energies of the two states we considered the initial and final state of those transitions. For further details on the theoretical approach used, we refer the reader to [19].

To a first approximation, the transition energy of the $2X^0$ state as a function of electric field is given by

$$\Delta E_{2X^0}(F) = E^0_{2X^0} - (\beta_{2X^0} - \beta_{1X^0}) \cdot \vec{F}^2 \qquad (2)$$

where $E^0_{2X^0}$ and β_{2X^0} denote the biexciton energy at zero electric field and the polarizability of the biexciton state, respectively. Comparison of the calculations shown in figure 2(c) with the extracted peak positions presented

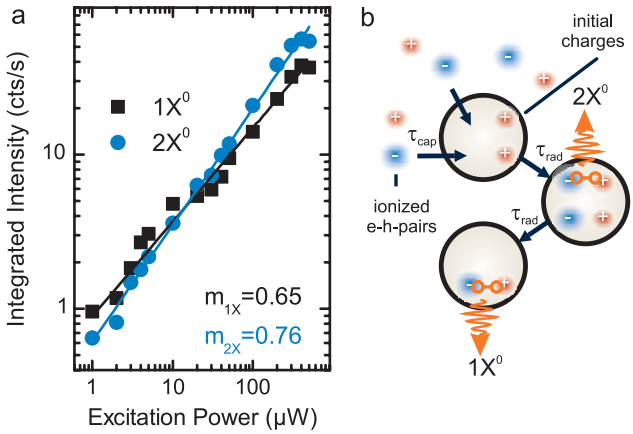

Figure 3. (a) PL intensity of $1X^0$ and $2X^0$ as a function of excitation power. (b) Schematic illustration of electron capture in initially charged QDs.

(This figure is in colour only in the electronic version)

in figure 2(b) shows qualitative agreement. Even the experimentally observed electric field $F_{res} \sim 17$ kV cm^{-1} where $1X^0$ and $2X^0$ can be tuned into resonance is close to the calculated value when we subtract the critical field $F_{crit} = 4.5$ kV cm^{-1} which is due to the screening, an effect not included in the calculations. However, the experimentally observed shift of the biexciton with electric field shows the opposite curvature compared to the calculations. This observation is, at present, not fully understood and remains subject to investigation.

We note that we cannot make a statement about any change of the exciton fine structure splitting as demonstrated, for example, in [9–11] due to the limited spectral resolution of our spectrometer.

The assignment of different emission lines of single QDs in PL studies is usually done via excitation power dependent measurements (as done for example in [20]). Here, one typically observes an approximately linear and quadratic behavior of the $1X^0$ and $2X^0$ emission lines, respectively. However, at $F = 7$ kV cm^{-1} we observe sub-linear behavior for both $1X^0$ and $2X^0$ with exponents of $m_{1X} = 0.65$ and $m_{2X} = 0.76$, respectively, as shown in figure 3(a). We attribute this unusual behavior to non-Poissonian statistics needed to describe the charge carrier capture processes at high electric fields. For electric fields $F > 3.3$ kV cm^{-1} ionization of optically excited e–h pairs occurs and, therefore, single electrons or holes are captured into the QD from the wetting layer rather than bound e–h pairs [17]. We obtain a rough estimation of the critical field by assuming that the ionization occurs when the potential energy $E_{pot} = -\vec{p} \cdot \vec{F}$ of the dipole $\vec{p}$ in an electric field $\vec{F}$ equals the exciton binding energy E_B. Thus, we obtain an expression for the critical field $F_{crit} = E_B/(e \cdot a_{ex})$, where e is the elementary charge of an electron and a_{ex} denotes the exciton binding radius. Using the exciton binding energy in InGaAs of $E_B = 6.3$ meV and a typical exciton binding radius of $a_{ex} = 18.9$ nm we obtain from this simple approximation a critical field of $F_{crit} = 3.3$ keV that is in good agreement with the value we determined

experimentally. This further explains the abrupt change in PL spectra at electric fields above F_{crit}, since either electrons or holes are preferentially captured in initially charged QDs, as schematically depicted in figure 3(b). In the case of an initially charged QD, one would preferentially capture electrons which leads to a reduction of Coulomb repulsion and, therefore, to a charge neutral dot in the biexciton states. In this case we would not observe linear and quadratic power dependence for excitons and biexcitons.

Nevertheless, there are strong indications that our attribution of the emission lines is correct. First of all the energy separation between exciton and biexciton $\Delta = 1.3$ meV is typical for the InGaAs QDs investigated here and in good agreement with other values reported in the literature [20, 21]. Furthermore, we observe excellent agreement between the measured DC Stark effect and theoretical calculations. Moreover, we performed the same experiments on many different QDs and samples and observed similar results for the exciton–biexciton detuning Δ, the power dependence and the Stark shift.

In conclusion, we have demonstrated a device consisting of single InGaAs QDs embedded in a lateral electric field geometry. The opposing quantum confined Stark shift for exciton and biexciton enables us to tune both emission lines in resonance at moderate electric fields $F \sim 17$ kV cm^{-1}. At resonance the biexciton–exciton radiative cascade is predicted to generate pairs of entangled photons provided there is time reordering of the emitted photons [13]. The problem of strongly decreasing PL intensity for increasing electric fields could be solved by exploiting the Purcell effect in photonic crystal microcavities [22].

Acknowledgments

We acknowledge the financial support of the Deutsche Forschungsgemeinschaft via the Sonderforschungsbereich 631, Teilprojekt B5, the Noether Programme (HJK) and the German Excellence Initiative via the 'Nanosystems Initiative Munich (NIM)'.

References

[1] Bouwmeester D *et al* 1997 *Nature* **390** 575
[2] Ekert A K 1991 *Phys. Rev. Lett.* **67** 661
[3] Benson O *et al* 2000 *Phys. Rev. Lett.* **84** 2513
[4] Stevenson R M *et al* 2006 *Nature* **439** 179
[5] Akopian N *et al* 2006 *Phys. Rev. Lett.* **96** 130501
[6] Hafenbrak R *et al* 2007 *New J. Phys.* **9** 315
[7] Santori C *et al* 2002 *Phys. Rev.* B **66** 045308
[8] Bayer M *et al* 1999 *Phys. Rev. Lett.* **82** 1748
[9] Gerardot B D *et al* 2007 *Appl. Phys. Lett.* **90** 041101
[10] Vogel M M *et al* 2007 *Appl. Phys. Lett.* **91** 051904
[11] Kowalik K *et al* 2007 *Appl. Phys. Lett.* **91** 183104
[12] Reimer M E *et al* 2008 *Phys. Rev.* B **78** 195301
[13] Avron J E *et al* 2008 *Phys. Rev. Lett.* **100** 120501
[14] Korkusinski M *et al* 2009 *Phys. Rev.* B **79** 035309
[15] Fry P W *et al* 2000 *Phys. Rev. Lett.* **84** 733
[16] For further information http://www.quickfield.com/
[17] Moskalenko E S *et al* 2006 *Phys. Rev.* B **73** 155336
[18] Krenner H J *et al* 2005 *New J. Phys.* **7** 184
[19] Rontani M *et al* 2001 *Solid State Commun.* **119** 309
[20] Finley J J *et al* 2001 *Phys. Rev.* B **63** 073307
[21] Heiss D *et al* 2009 *Appl. Phys. Lett.* **94** 072108
[22] Kress A *et al* 2005 *Phys. Rev.* B **71** 241304(R)